High-Energy Spin Excitations in the Electron-Doped Superconductor $Pr_{0.88}LaCe_{0.12}CuO_{4-\delta}$ with $T_c = 21$ K

Stephen D. Wilson,[1] Shiliang Li,[1] Hyungje Woo,[1] Pengcheng Dai,[1,2,*] H. A. Mook,[2] C. D. Frost,[3] Seiki Komiya,[4] and Yoichi Ando[4]

[1]*Department of Physics and Astronomy, The University of Tennessee, Knoxville, Tennessee 37996-1200, USA*
[2]*Center for Neutron Scattering, Oak Ridge National Laboratory, Oak Ridge, Tennessee 37831-6393, USA*
[3]*ISIS Facility, Rutherford Appleton Laboratory, Oxon OX11 0QX, United Kingdom*
[4]*Central Research Institute of Electric Power Industry, Komae, Tokyo 201-8511, Japan*

(Received 10 October 2005; published 18 April 2006)

We use high-resolution inelastic neutron scattering to study the low-temperature magnetic excitations of the electron-doping superconductor $Pr_{0.88}LaCe_{0.12}CuO_{4-\delta}$ ($T_c = 21 \pm 1$ K) over a wide energy range (4 meV $\leq \hbar\omega \leq$ 330 meV). The effect of electron doping is to cause a wave vector (Q) broadening in the low-energy ($\hbar\omega \leq 80$ meV) commensurate spin fluctuations at (0.5, 0.5) and to suppress the intensity of spin-wave-like excitations at high energies ($\hbar\omega \geq 100$ meV). This leads to a substantial redistribution in the spectrum of the local dynamical spin susceptibility $\chi''(\omega)$, and reveals a new energy scale similar to that of the lightly hole-doped $YB_2Cu_3O_{6.353}$ ($T_c = 18$ K).

DOI: 10.1103/PhysRevLett.96.157001 PACS numbers: 74.72.Jt, 61.12.Ld, 75.25.+z

High-transition-temperature (high-T_c) superconductivity in copper oxides occurs when sufficient holes or electrons are doped into the CuO_2 planes of their insulating antiferromagnetic (AF) parent compounds [1]. Given the close proximity of AF order and superconductivity, it is important to understand the evolution of magnetic excitations in the parent insulators upon chemical doping to produce metals and superconductors, as spin fluctuations may play a crucial role in the mechanism of superconductivity [2]. For the undoped parent compounds, where AF order gives a diffraction peak at wave vector (0.5, 0.5) [Fig. 1(a)], spin waves at energies ($\hbar\omega$) below 60 meV found by neutron scattering show commensurate excitations around (0.5, 0.5) because of the large AF nearest-neighbor exchange coupling [$J_1 > 100$ meV, Figs. 1(a), 1(c), and 3(a)] [3–5]. Upon hole doping to induce metallicity and superconductivity, the low-energy spin fluctuations of $La_{2-x}(Sr, Br)_xCuO_4$ (LSCO) form a quartet of incommensurate peaks at wave vectors away from (0.5, 0.5) [6–8] that may arise from the presence of static or dynamic spin stripes [9]. For hole-doped $YBa_2Cu_3O_{6+x}$ (YBCO) with $x \geq 0.45$, the magnetic excitation spectra have a commensurate resonance and incommensurate spin fluctuations similar to that of LSCO below this resonance [10–15]. For energies above the resonance, the excitations are spin-wave-like for $x \leq 0.5$ [13,15] but become a "box-like" at $x = 0.6$ [14]. In the extremely underdoped regime ($x = 0.353$, $T_c = 18$ K), Stock *et al.* [16] showed that spin fluctuations are commensurate around (0.5, 0.5) and have a damped spin resonance around 2 meV.

While the evolution of spin excitations in hole-doped superconductors has become increasingly clear, it is crucial to determine the evolution of spin excitations in electron-doped materials, as particle-hole symmetry is an important ingredient of any theory purporting to explain the mechanism of high-T_c superconductivity. Unfortunately, due to the difficulty of growing large single crystals required for inelastic neutron scattering experiments, there exist only a few studies exploring the low-energy ($\hbar\omega \leq 10$ meV) spin dynamics in electron-doped

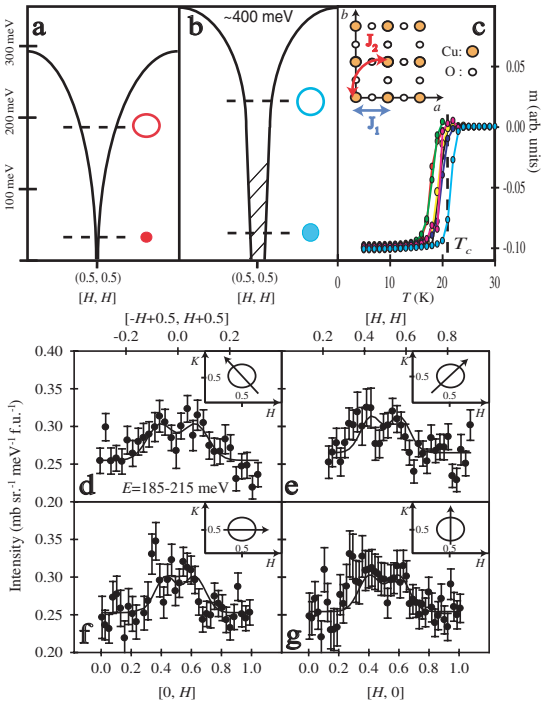

FIG. 1 (color online). Pictorial representation of the dispersions of the spin excitations in the (a) insulating Pr_2CuO_4 and (b) superconducting PLCCO. (c) Magnetic susceptibility measurements of T_c's in arbitrary units for the seven samples. The inset shows the unit cell with exchange couplings J_1 and J_2. (d), (e), (f), (g) one-dimensional cuts through the spin excitations at $\hbar\omega = 200 \pm 15$ meV along the $[\bar{1}, 1]$, [1,1], [1,0], [0,1] directions.

$Nd_{1.85}Ce_{0.15}CuO_4$ (NCCO) [17], and consequently the overall magnetic response of electron-doping materials remains largely unknown. Recently, we began to systematically investigate the evolution of AF order and magnetic excitations as $Pr_{0.88}LaCe_{0.12}CuO_{4-\delta}$ (PLCCO) is transformed from the as-grown AF insulator into an optimally electron-doped superconductor ($T_c = 25$ K) through an annealing process with a minor oxygen content δ modification [18–20]. We chose first to study underdoped PLCCO ($T_c \sim 21$ K) with weak static AF order ($T_N \sim 40$ K with Cu ordered moment of $\sim 0.04 \mu_B$) because this material has a larger magnetic signal than that of the optimally doped PLCCO [18–21].

In this Letter, we report the results of inelastic neutron scattering measurements that probe the low-temperature ($T = 7$ K) dynamic spin response of PLCCO ($T_c = 21 \pm 1$ K) for energies from 4 meV to 330 meV. We determine the Q and ω dependence of the generalized magnetic susceptibility $\chi''(\mathbf{Q}, \omega)$ [3]. We find that the effect of electron doping into the AF insulating PLCCO is to cause a wave vector broadening in the low-energy commensurate magnetic excitations at (0.5, 0.5) [17]. At high energies ($\hbar\omega \geq 100$ meV), the excitations are spin-wave-like rings, but with a dispersion steeper than that of the undoped Pr_2CuO_4 [4] and a significant reduction in the spectral weight of the local dynamical spin susceptibility $\chi''(\omega)$ [3]. A comparison of PLCCO and lightly doped YBCO ($x = 0.353$) [16] reveals that the energy scale for $\chi''(\omega)$ in both materials is at ~ 2 meV, lower than the ~ 18 meV for the optimally doped LSCO [8].

We grew seven high quality (mosaicity $<1°$) PLCCO single crystals (with a total mass of 20.5 g) using a mirror image furnace. To obtain superconductivity, we annealed the as-grown nonsuperconducting samples in a vacuum ($P < 10^{-6}$ mbar) at $T = 765 \pm 1\,°C$ for four days. While both ends of the same crystal were found to have identical T_c's, there are small (± 1 K) differences in T_c's for separately annealed samples. Figure 1(c) shows magnetic susceptibility measurements on all seven crystals used in our neutron experiments ($T_c = 21 \pm 1$ K). For the experiment, we define the wave vector $\mathbf{Q}$ at (q_x, q_y, q_z) as $(H, K, L) = (q_x a/2\pi, q_y a/2\pi, q_z c/2\pi)$ reciprocal lattice units (r.l.u.) in the tetragonal unit cell of PLCCO (space group $I4/mmm$, $a = 3.98$, and $c = 12.27$ Å). The seven PLCCO crystals were coaligned to within 1° in the $[H, H, L]$ zone using HB-1/HB-1A triple axis spectrometers at the High-Flux-Isotope reactor, Oak Ridge National Laboratory. Our inelastic neutron scattering experiments were performed on the MAPS time-of-flight spectrometer with the incident beam parallel to the c axis (L direction) of PLCCO at the ISIS facility [14]. Four different incident beam energies of $E_i = 40$, 115, 200, and 400 meV were used, and the scattering was normalized to absolute units using a vanadium standard.

Figure 2 summarizes images of neutron scattering intensity $S(\mathbf{Q}, \omega)$ centered about (0.5, 0.5) at $T = 7$ K in

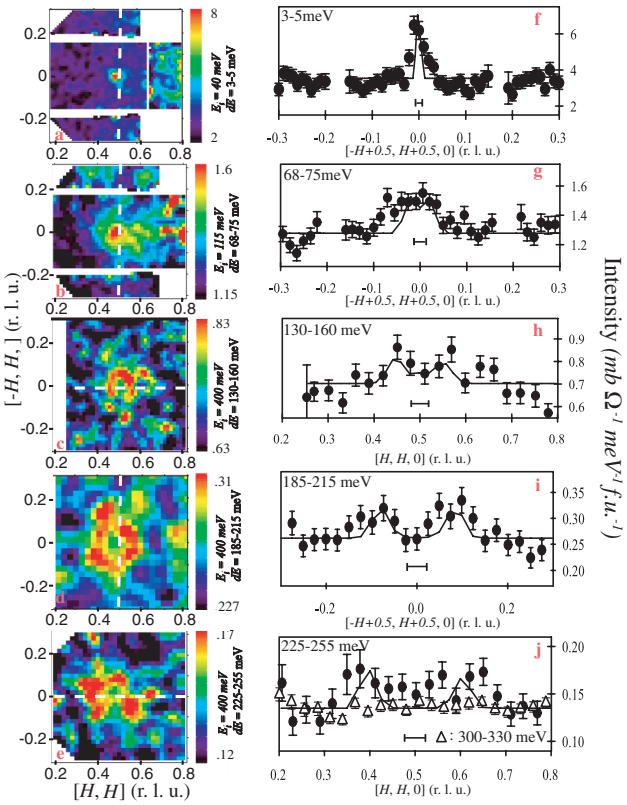

FIG. 2 (color online). $S(\mathbf{Q}, \omega)$ in the (H, K) plane at (a) $\hbar\omega = 4 \pm 1$, (b) 71.5 ± 3.5, (c) 150 ± 10, (d) 200 ± 15, and (e) 240 ± 15 meV. The incident beam energy $E_i = 40$, 115, 200, and 400 meV data have counting times of 18, 60, 44, and 76 hours, respectively, with a source proton current of 170 μA. (f), (g), (h), (i), (j) $\mathbf{Q}$ cuts passing through (0.5, 0.5) along the dashed line directions shown in (a), (b), (c), (d), (e). Upper open triangles in (j) show a cut at $\hbar\omega = 315 \pm 15$ meV along the [1,1] direction. Solid lines are the calculated one-magnon cross sections from the linear spin wave fit to the data with $J_1 = 162$ meV and $J_2 = 0$. Horizontal bars below each cut show the instrumental resolution.

units of mbarns/sr/meV/f.u. without any background subtraction. At the lowest energy ($\hbar\omega = 4 \pm 1$ meV) probed [Fig. 2(a)], the scattering consists of a strong peak at (0.5, 0.5) with some phonon contamination evident at larger wave vectors. A cut through the image reveals a commensurate peak on a flat background [Fig. 2(f)]. The peak is significantly broader than the instrumental resolution (horizontal bar) and gives a correlation length of ~ 70 Å. Upon increasing energy, the peak broadens in width [Fig. 2(b)] and weakens in intensity [Fig. 2(g)]. With further increase in energy to $\hbar\omega = 145 \pm 15$ meV, the scattering becomes a spin-wave-like ring [Figs. 2(c) and 2(h)]. One-dimensional cuts through Fig. 2(d) at $\hbar\omega = 200 \pm 15$ meV along four different directions [Figs. 1(d)–1(g)] confirm that the scattering is indeed isotropic and symmetric around (0.5, 0.5)-like spin waves. With increasing energy, the ring continues to disperse outward until magnetic scattering is no longer discernible at $\hbar\omega = 315 \pm 15$ meV [Fig. 2(j)].

Figure 3(a) summarizes the dispersion of spin excitations determined from the cuts in Figs. 2(f)–2(j). The dashed boxes show the positions of crystalline electric field (CEF) excitations arising from the Pr^{3+} ions in the tetragonal structure of PLCCO [22]. Compared to intensities of Pr^{3+} CEF levels, Cu^{2+} spin fluctuations in PLCCO are extremely weak and cannot be separated from the strong Pr^{3+} scattering at certain CEF energy positions. For reference, Fig. 3(b) shows an energy cut along $\mathbf{Q} = (0.5, 0.5, L)$ for the $E_i = 115$ meV data. It is clear that CEF intensities at $\hbar\omega \approx 20, 85$ meV are significant relative even to the incoherent elastic scattering.

To estimate the strength of the magnetic exchange coupling, we consider a two-dimensional AF Heisenberg Hamiltonian with the nearest (J_1) and the next nearest (J_2) neighbor coupling [Fig. 1(c)]. Since the zone boundary spin fluctuations sensitive to J_2 were unobservable [Fig. 2(j)], we set $J_2 = 0$ and determined that $J_1 = 162 \pm 13$ meV renders the best fit to the data for $\hbar\omega \geq 100$ meV. The corresponding calculated one-magnon cross sections are plotted as the solid lines in Figs. 2(h)–2(j), and the resulting dispersion relation is shown as the solid line in Fig. 3(a). At high energies ($\hbar\omega \geq 100$ meV), the calculated spin-wave dispersion coincides fairly well with the data, but the value of J_1 is considerably larger than the hole-doped (La_2CuO_4, $J_1 = 104$, $J_2 = -18$ meV) [5] and electron-doped (Pr_2CuO_4, $J_1 = 121$ meV) [4] parent compounds [Fig. 3(a)]. Assuming as-grown insulating PLCCO has similar AF exchange coupling as Pr_2CuO_4 [4], our data suggest that the high-energy spin fluctuations in electron-doping PLCCO disperse faster than the spin waves of the insulating compound. Therefore, they are unlikely to arise from the weak static AF order in the material [18].

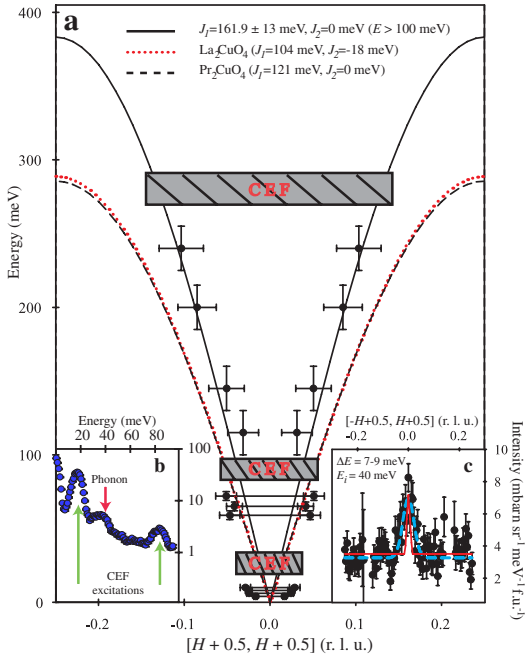

FIG. 3 (color online). (a) The dispersion of spin excitations in PLCCO. Points connected by solid lines denote peaks centered around (0.5, 0.5) and represent the FWHM of a Gaussian fit with the instrument resolution deconvoluted. Solid, dotted, and dashed lines show dispersions from linear spin-wave fits with various exchange couplings. (b) Log vs linear energy cut averaged from $H = 0.45$ to 0.55 along the [1,1] direction and from $H = -0.05$ to 0.05 along the $[\bar{1}, 1]$ direction. CEF and phonon contamination energies are marked by arrows. (c) $\mathbf{Q}$ cut along the $[\bar{1}, 1]$ direction with $\hbar\omega = 8 \pm 1$ meV with a Gaussian fit in a dashed line (blue online) and the calculated one-magnon cross section in solid (red online) with $J = 121$ meV.

Although high-energy spin excitations in PLCCO are spin-wave-like, the observed scattering for $\hbar\omega \leq 80$ meV is substantially broader than those predicted by the linear spin-wave theory [Fig. 3(a)]. A cut at $\hbar\omega = 8 \pm 1$ meV through the (0.5, 0.5) point along the $[\bar{1}, 1]$ direction confirms this point [Fig. 3(c)]. Therefore, the dispersion of PLCCO can be separated into two regimes. For energies ($4 \leq \hbar\omega \leq 80$ meV), the excitations are broad and weakly dispersive. For $\hbar\omega \geq 100$ meV, the fluctuations are spin-wave-like with J_1 larger than that of the insulating parent compound.

In addition to determining the dispersion of spin excitations in PLCCO, the absolute spin susceptibility $\chi''(\mathbf{Q}, \omega)$ measurements in Fig. 2 also allow us to calculate the energy dependence of the local susceptibility $\chi''(\omega)$, defined as $\int \chi''(\mathbf{Q}, \omega) d^3Q / \int d^3Q$ [23,24]. Figure 4 (main

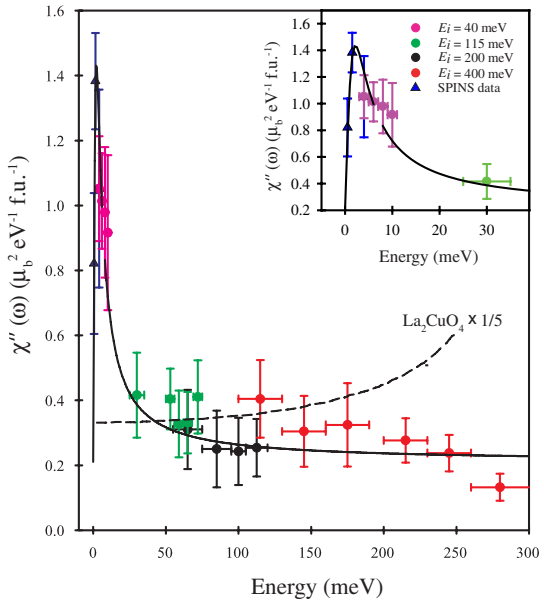

FIG. 4 (color online). Energy dependence of local susceptibility $\chi''(\omega)$ in PLCCO determined from integration over the magnetic scattering around (0.5, 0.5) [23,24]. The dashed line shows $\chi''(\omega) \times 1/5$ for La_2CuO_4 [3]. Since $\mathbf{Q}$ cuts were made along the $[\bar{1}, 1]$ direction, the background scattering can be approximated by a constant. The triangles (blue online) indicate normalized SPINS data on a $T_c = 21$ K PLCCO sample at energies below 3 meV [20]. The inset shows an expanded view of $\chi''(\omega)$ vs $\hbar\omega$ at low energies. The solid line is a damped Lorenztian on a constant background.

figure) shows how $\chi''(\omega)$ varies as a function of $\hbar\omega$ for PLCCO. Similar to hole-doped materials [3,7,8,14–16], electron doping suppresses the spectral weight of spin fluctuations in PLCCO at high (≥ 50 meV) energies. For energies below 50 meV, $\chi''(\omega)$ increases with decreasing energy and does not saturate at $\hbar\omega = 4 \pm 1$ meV, the lowest energy probed on MAPS. Assuming that the $\chi''(\omega)$ in crystals of MAPS experiments ($T_c = 21 \pm 1$ K) is similar to that of the previously studied $T_c = 21$ K PLCCO sample [18–20], we can normalize the low-energy magnetic response of the $T_c = 21$ K sample obtained on SPINS spectrometer at NIST to that of the MAPS data. The outcome, shown as inset of Fig. 4, reveals a new energy scale of 2–3 meV for PLCCO.

We are now in a position to compare the spin excitations of electron-doping PLCCO with that of the hole-doped LSCO [7,8] and YBCO [13–16,24]. For hole-doped materials such as LSCO [6–8] and YBCO with $x \geq 0.45$ [12–15], the low-energy spin fluctuations are incommensurate and display an inward dispersion toward a resonance point with increasing energy. This is not observed in electron-doped materials. Instead, spin fluctuations in PLCCO have a broad commensurate peak centered at (0.5, 0.5) at low-energies (≤ 50 meV) which disperses outward into a continuous spin-wave, ring-like scattering at high energies (≥ 100 meV), similar to the lightly doped YBCO ($x = 0.353$) [16]. At present, it is not clear how theoretical models based on spin stripes [9] can reconcile the differences in spin excitations between the hole- and electron-doping materials.

For hole-doped LSCO with $T_c = 38.5$ K, the mean-squared fluctuating moment $\langle m^2 \rangle = \int \chi''(\omega) d\omega$ integrated up to 40 meV is $\langle m^2 \rangle = 0.062 \pm 0.005 \mu_B^2$ f.u.$^{-1}$ [8]. For comparison, $\langle m^2 \rangle$ calculated from $\chi''(\omega)$ up to 40 meV is only $0.024 \pm 0.003 \mu_B^2$ f.u.$^{-1}$ in PLCCO, about 3 times smaller than that of LSCO. The total fluctuating moment integrated from 0 to 300 meV (Fig. 4) gives $\langle m^2 \rangle = 0.089 \pm 0.009 \mu_B^2$ f.u.$^{-1}$, a value an the order of a magnitude larger than the static moment squared of the $T_c = 21$ K PLCCO ($0.0016 \mu_B^2$ f.u.$^{-1}$) [18]. Since the total moment sum rule for the spin-$\frac{1}{2}$ Heisenberg model requires the integrated one-magnon fluctuating moment squared to be smaller than the ordered moment squared [25], the observed high-energy spin-wave-like excitations are unlikely to arise from the small ordered moment.

In the standard Hubbard model and its strong-coupling limit, the t-J model with only the nearest-neighbor hopping t, there should be complete particle-hole symmetry and therefore the electron- and hole-doped copper oxides should behave identically. The observed large difference between incommensurate and commensurate spin fluctuations in hole- [6–8] and electron-doping materials [17–20] has mostly been attributed to their differences in the strength of second nearest-neighbor (t') and third (t'') nearest-neighbor hopping. This also explains their differences in Fermi surface topology within the t-J model [26–28], although it may also be due to their proximity to two different quantum critical points [29]. In the most recent calculation using the slave-boson mean-field theory and random phase approximation [28], incommensurate spin fluctuations at (0.3, 0.7) have been predicted for optimally doped NCCO. However, this is not observed in our PLCCO [Figs. 2(a)–2(e)]. Similarly, the energy dependence of the $\chi''(\mathbf{Q}, \omega)$ at $\mathbf{Q} = (0.5, 0.5)$ has been predicted to exhibit a peak between $0.1\omega/J$ [26,28] and $0.4\omega/J$ [27]. While qualitatively similar to the predictions, $\chi''(\omega)$ in Fig. 4 has a peak at a much smaller energy of $0.02\omega/J$. Comparison of future calculations in absolute units with our data should determine whether itinerant magnetism models can account quantitatively for the observed dynamic susceptibility in superconducting PLCCO.

S. W. and S. L. are supported by the U.S. NSF Grant No. DMR-0453804, H. W. is supported by the DOE BES Grant No. DE-FG02-05ER46202. This work is also supported by DOE Grant No. DE-AC05-00OR22725 with UT/Battelle LLC and by the Grant-in-Aid for Science from JSPS.

*Electronic address: daip@ornl.gov

[1] M. A. Kastner *et al.*, Rev. Mod. Phys. **70**, 897 (1998).
[2] D. J. Scalapino, Science **284**, 1282 (1999).
[3] S. M. Hayden *et al.*, Phys. Rev. Lett. **76**, 1344 (1996).
[4] P. Bourges *et al.*, Phys. Rev. Lett. **79**, 4906 (1997).
[5] R. Coldea *et al.*, Phys. Rev. Lett. **86**, 5377 (2001).
[6] S.-W. Cheong *et al.*, Phys. Rev. Lett. **67**, 1791 (1991).
[7] J. M. Tranquada *et al.*, Nature (London) **429**, 534 (2004).
[8] N. B. Christensen *et al.*, Phys. Rev. Lett. **93**, 147002 (2004).
[9] S. A. Kivelson *et al.*, Rev. Mod. Phys. **75**, 1201 (2003).
[10] J. Rossat-Mignod *et al.*, Physica (Amsterdam) **185C**, 86 (1991).
[11] H. F. Fong *et al.*, Phys. Rev. B **61**, 14 773 (2000).
[12] Pengcheng Dai *et al.*, Phys. Rev. B **63**, 054525 (2001).
[13] P. Bourges *et al.*, Phys. Rev. B **56**, R11439 (1997).
[14] S. M. Hayden *et al.*, Nature (London) **429**, 531 (2004).
[15] C. Stock *et al.*, Phys. Rev. B **71**, 024522 (2005).
[16] C. Stock *et al.*, Phys. Rev. B **73**, 100504(R) (2006).
[17] K. Yamada *et al.*, Phys. Rev. Lett. **90**, 137004 (2003).
[18] Pengcheng Dai *et al.*, Phys. Rev. B **71**, 100502 (2005).
[19] H. J. Kang *et al.*, Phys. Rev. B **71**, 214512 (2005).
[20] S. D. Wilson *et al.* (unpublished).
[21] M. Fujita *et al.*, Phys. Rev. B **67**, 014514 (2003).
[22] A. T. Boothroyd *et al.*, Phys. Rev. B **45**, 10 075 (1992).
[23] S. M. Hayden *et al.*, Physica (Amsterdam) **241–243B**, 765 (1998).
[24] Pengcheng Dai *et al.*, Science **284**, 1344 (1999).
[25] J. Lorenzana *et al.*, Phys. Rev. B **72**, 224511 (2005).
[26] Jian-Xin Li *et al.*, Phys. Rev. B **68**, 224503 (2003).
[27] T. Tohyama, Phys. Rev. B **70**, 174517 (2004).
[28] Quingshan Yuan *et al.*, Phys. Rev. B **71**, 134522 (2005).
[29] F. Onufrieva and P. Pfeuty, Phys. Rev. Lett. **92**, 247003 (2004).